Supplementary Information

Intelligent Acoustofluidics Enabled Mini-bioreactors for Human Brain Organoids

Hongwei Cai,[1] Zheng Ao,[1] Zhuhao Wu,[1] Sunghwa Song,[1] Ken Mackie,[2] and Feng Guo,[1,]*

1. Department of Intelligent Systems Engineering, Indiana University, Bloomington, IN 47405, United States
2. Gill Center for Biomolecular Science, and Department of Psychological and Brain Sciences, Indiana University, Bloomington, IN 47405, United States

*Corresponding email: fengguo@iu.edu

Supporting statement:

Supporting Figures:

Figure S1. Acoustic spiral phase device and simulation domain.

Supporting Movie:

Movie S1. Rotation under a sudden weight load.

Supporting Tables:

Table S1. Antibody for immunofluorescence staining
Table S2. Primer sequences for qPCR analysis

Supporting statement (Acoustic vortex field simulation and torque calculation):

A simulation model was developed to account for the acoustic vortex field bypass the acoustic spiral phase plate (ASPP). The simulation was conducted using the finite element package COMSOL 5.2a (COMSOL group). The model domain established for the numerical simulation is shown in **Figure S1a**. The background medium is defined as the water with a mass density of 1000 kg/m³ and sound speed of 1490 m/s, while the ASPP is defined as 3D printed materials (PLA) with a mass density of 1190 kg/m³ and sound speed of 2200 m/s. To simplify the simulation and reduce the computational cost, we only considered longitudinal sound waves vibrating along the normal direction of the ASPP. The "Pressure Acoustic" physics module was used to solve the acoustic pressure and phase-field distribution. The plane wave radiation boundary condition and incident waves condition was imposed on the incident boundary to introduce acoustic waves and absorb the reflected waves. The sound hard boundary condition was assumed on the side boundaries of the cylindrical water domain. To ensure the simulation accuracy, one-tenth of the acoustic wavelength in water was set to be the maximum mesh element size, the meshes were further refined in the ASPP units.

As the ASPP converts plane incident waves to an acoustic vortex field, a torque also applies to the ASPP and drives the ASPP to rotate. The torque applied to the ASPP can be described following basic continuum mechanics, including acoustic absorption by the ASPP and the reflected acoustic field by the ASPP spiral surface. The acoustic radiation stress along the ASPP surface exsert the torque. In the case of an ideal ASPP (**Figure S1b**), the torque can be written as:

$$f(r,\phi) \propto \frac{I(r)}{c_2}[(1 + R(r))cos^2\beta(r) - \frac{c_2}{c_1}T(r)cos^2\gamma(r)]n_{2\to1}$$

where $\gamma = arcsin[(c_1/c_2)sin\beta]$ is the refraction angle, $\beta = arctan[l\varepsilon/(2\pi r)]$ is the local inclination angle with respect to the spiral axis, l an integer for the topological charge, $\varepsilon = \dfrac{1}{f(c_1^{-1} - c_2^{-1})}$, $I(r)$ is the local acoustic intensity of the incident acoustic waves, $T = (4Z_1/Z_2)/(Z_1/Z_2 + cos\gamma/cos\beta)^2$ represents the transmittance, $Z_i = \rho_i c_i$ the acoustic impedances of water ($i = 1$) and PLA ($i = 2$), ρ is the mass density, $R = 1 - cos\gamma/cos\beta \, T$ is the reflectance. The total torque Γ applied to the ASPP can be calculated by integrating the torque density among the ASPP ramp surface $\Gamma = \displaystyle\int_0^{2\pi}\int_0^{R} ru_r \times f \, r dr d\phi$, where (u_r, u_ϕ, u_z) refers to the cylindrical coordinate system.
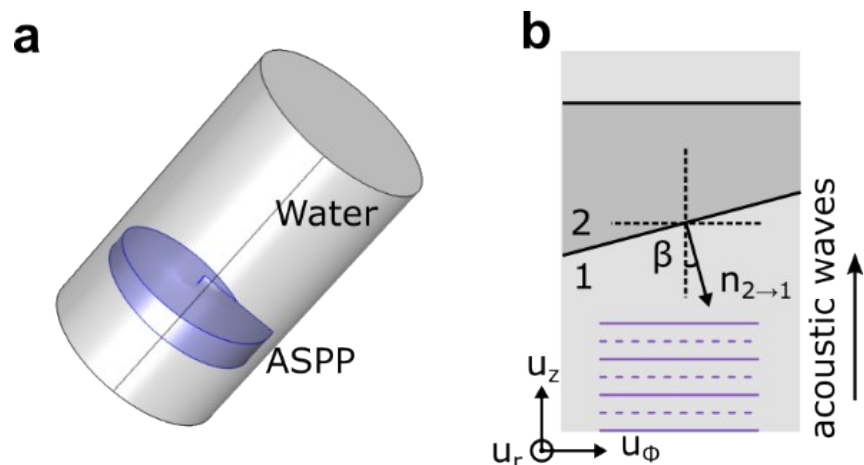
Figure S1. Acoustic field simulation domain and torque calculation. (a) Simulation domain of the acoustic spiral phase plate, the blue part is the ASPP with topological charge $l = 1$. (b) Local representative schematic of incident waves transmission and reflection.
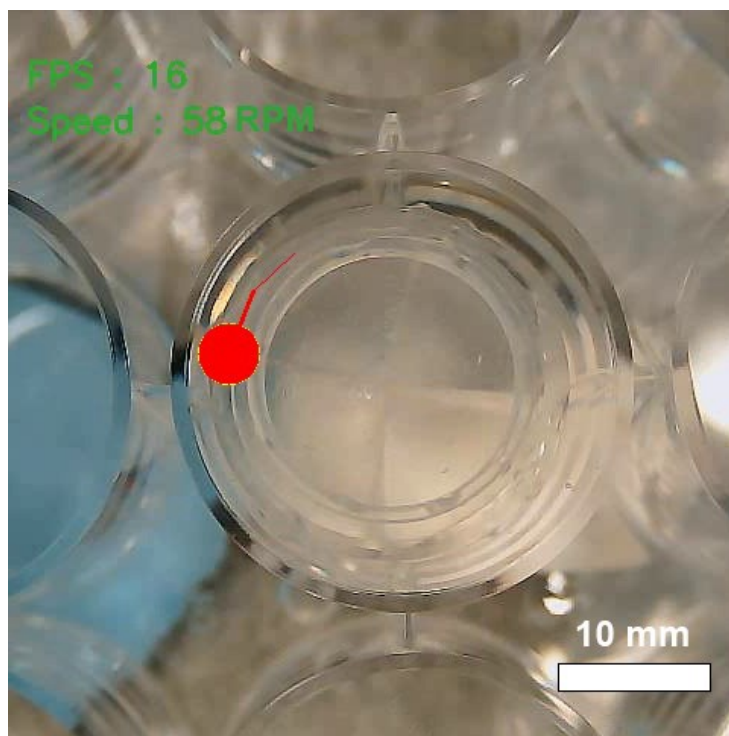
Movie S1. Rotational stability under sudden weight load disturbance (corresponding to Figure 4d). The movie is in real-time. (Scale bar: 500 μm).

Table S1. Antibody for immunofluorescence staining

Antigen	Host	Vendor	Catalog#	Dilution
Pax6	Rabbit	Biolegend	901301	1:500
Map2	Chicken	Millipore	AB5543	1:500

Table S2. Primer sequences for qPCR analysis

Gene	Primer sequence
PAX6 Fwd	AGT TCT TCG CAA CCT GGC TA
PAX6 Rev	ATT CTC TCC CCC TCC TTC CT
TBR1 Fwd	GAC TCA GTT CAT CGC CGT CA
TBR1 Rev	TCG TGT CAT AAT TAT CCC GAA ATC C
CTIP2 Fwd	CAG AGC AGC AAG CTC ACG
CTIP2 Rev	GGT GCT GTA GAC GCT GAA GG
NKX2.1 Fwd	GGA GGG AGC TGG GGA GAG G
NKX2.1 Rev	ATT TTC GCG GAG GGC GGT CG
OTX-2 Fwd	TTA AAA TCT CTG CCA TGG AAA
OTX-2 Rev	AGA ACA AAA ACC CGT GCC TT
En2 Fwd	GAA CCC GAA CAA AGA GGA CA
En2 Rev	CGC TTG TTC TGG AAC CAA AT
Brachyury Fwd	CCC GTC TCC TTC AGC AAA GTC
Brachyury Rev	TGG ATT CGA GGC TCA TAC TTA TGC
SOX17 Fwd	AGA TGC TGG GCA AGT CGT
SOX17 Rev	GCT TCA GCC GCT TCA CC